Mapping Class I Methanol Masers in the DR21 Region

Talitha Muehlbrad
Texas Lutheran University, MIT Haystack REU Program

Introduction

Masers are used in astronomy as probes for conditions in interstellar clouds. They can be used to study temperatures, densities, magnetic fields, and outflows. Methanol masers are divided into two groups: Class I and Class II. Class I masers are usually found in massive star forming regions, and are believed to be formed by collisional pumping due to shocks. They are found apart from ultracompact HII regions and IR sources. Class I and II masers are usually found apart from each other.

The region we observed is DR21. DR21 is a massive star forming region in our galaxy. The images below were taken by SPITZER and show false color maps of the region.

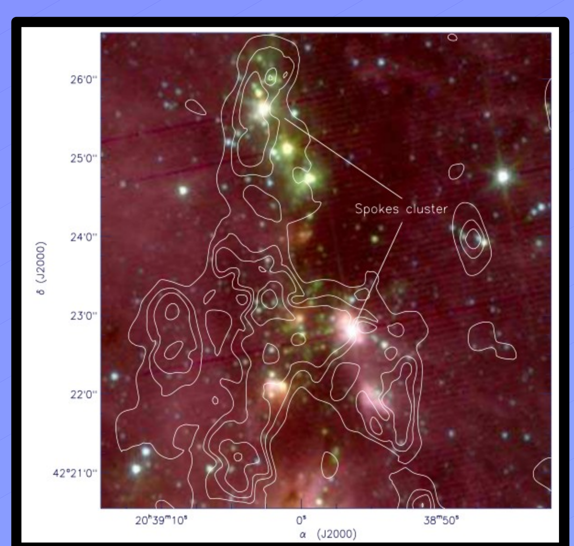

Region around DR21OH
Kumar et al, 2007

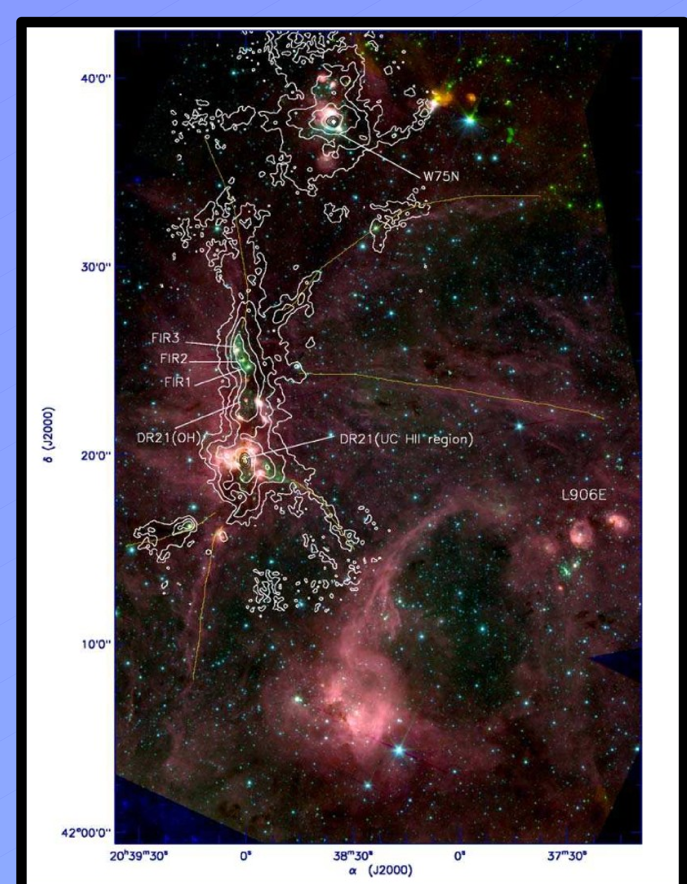

(Right) A color image of the full DR21/W75 mosaic observed with the Spitzer Space Telescope, composed from images in 3.6 µm (blue), 4.5 µm (green) and 8.0 µm (red). Contours represent the 850-µm emission mapped using SCUBA on JCMT. (Kumar et al, 2007)

Observations

Using the Expanded Very Large Array (EVLA) in Socorro, NM, we observed the 36.169265 Ghz $4_{-1} \rightarrow 3_0$ *E* transition line of methanol masers in three areas of the massive star forming region DR21. The three areas observed were DR21OH, DR21N, and DR21W. Data were taken with the EVLA in D configuration. Once the data was cleaned and processed using AIPS, each maser detection was examined and fitted with Gaussian parameters across the bandwidth. The masers spots were plotted on velocity maps against known masers in other transitions in the same region. Observations were taken across a bandwidth of 4 MHz in 256 spectral channels, giving a velocity range of 33.1 km s^{-1} and a velocity resolution of 0.13 km s^{-1}. The observed field had a radius of 50 arcseconds, displayed across 256-pixel radius. AIPS was used for data reduction.

DR21OH

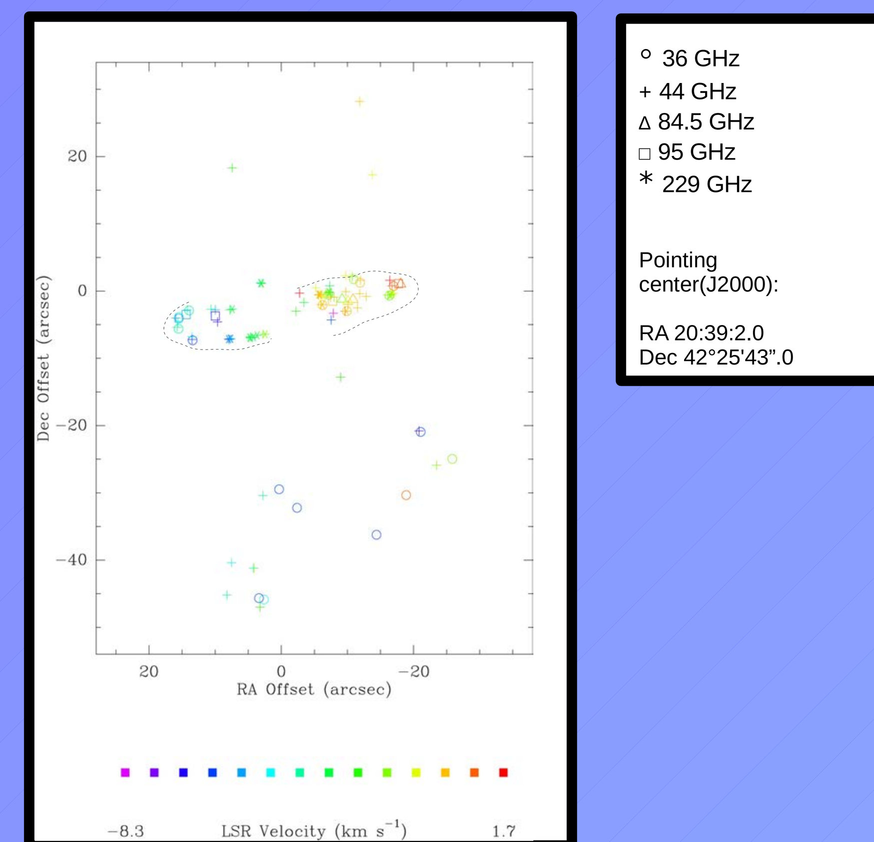

The figure on the left shows our 36 GHz data plotted against maser detections in the 44 (Araya et al, 2009), 84.5 (Batrla and Menten, 1988), 95 (Plambeck and Menten, 1990), and 226 GHz transitions (Bourke and Pratap, in preparation). Notice the double-arc structure present in each transition (outlined in figure). These "wings" are mostly likely tracing an outflow and the source is probably a young massive stellar object near the center. The arc-like patterns suggest bow-shock origins.

There are some 44 GHz detections to the north of the outflow and some 44 and 36 GHz detections to the south. In some places, the two transitions are similar in space and velocity.

DR21N

This source had no interferometric maps of other transitions to which our data could be compared, though Pratap's 2008 paper indicates a strong methanol emission line in the 44GHz transition. The pattern here shows no clear organization. The spots on the eastern side are large clusters of low-intensity (0.15-1.63 Jy) blue-shifted masers, while the western side is a rough line of brighter, redshifted masers (near dotted line). There is also a single very blue-shifted maser just north of this line. Several of the low-intensity masers show extended emission, which given the close clustering in the area, is most likely an indication of multiple masers which cannot be resolved with our observations.

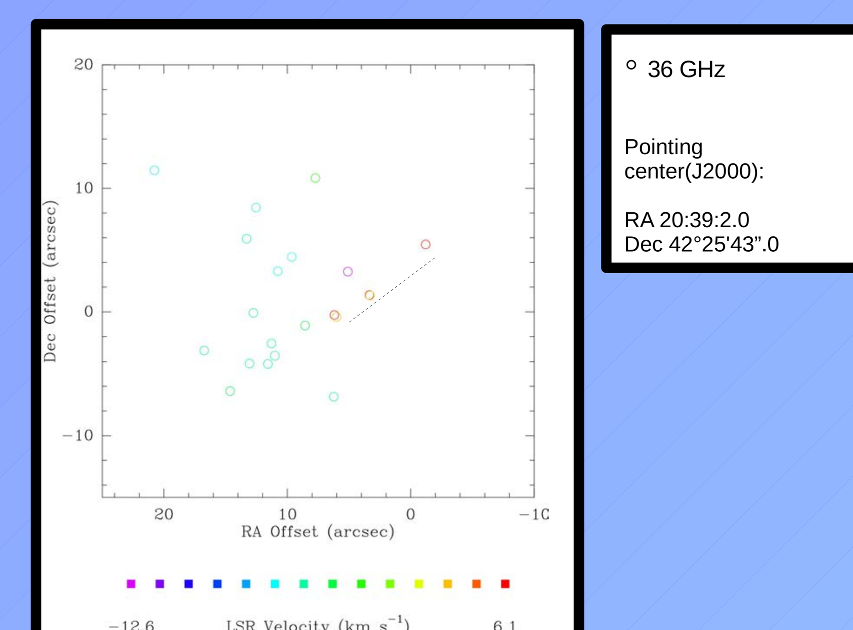

DR21W

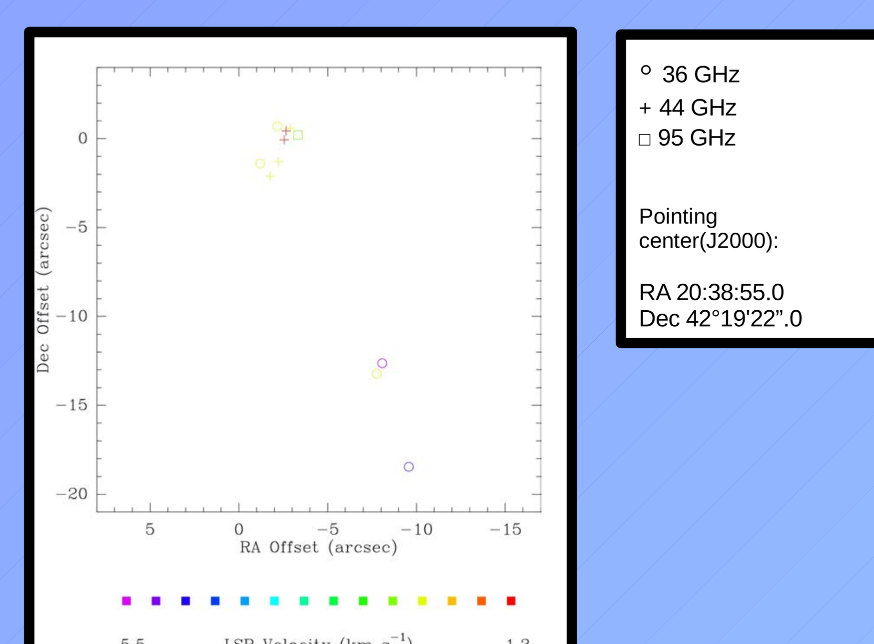

Our 36 GHz detections are plotted against 44 GHz detections by Kogan and Slysh (1998) and 95 GHz detections by Plambeck and Menten (1990). In the northeast corner, the three data sets appear to align almost on top of one another. There is a slight positional offset, but due to the varying angular resolutions, it is highly plausible that the sets are even closer.

The velocities of the different transitions are also very similar, within error in most cases. The error here is comprised of the error in the center velocity and the uncertainties in the rest frequencies. Of the masers displayed in the line, only two of the 44 GHz masers show a significant velocity offset outside of the error (~1 km s^{-1} difference).

Zeeman Splitting and Evidence for a Different Pumping Mechanism

Zeeman Splitting

Zeeman splitting is used to detect the magnetic field within a region. Sarma and Momjian reported the first detection of the Zeeman for 36 GHz masers in 2009. Following their methods, we were also able to use the effect to report a magnetic field in one of our sources. The magnetic field measurement is obtained by examining the Stokes *V* spectrum as a function of Stokes *I*:

$$V = aI + \frac{b}{2}\frac{dI}{dv}$$

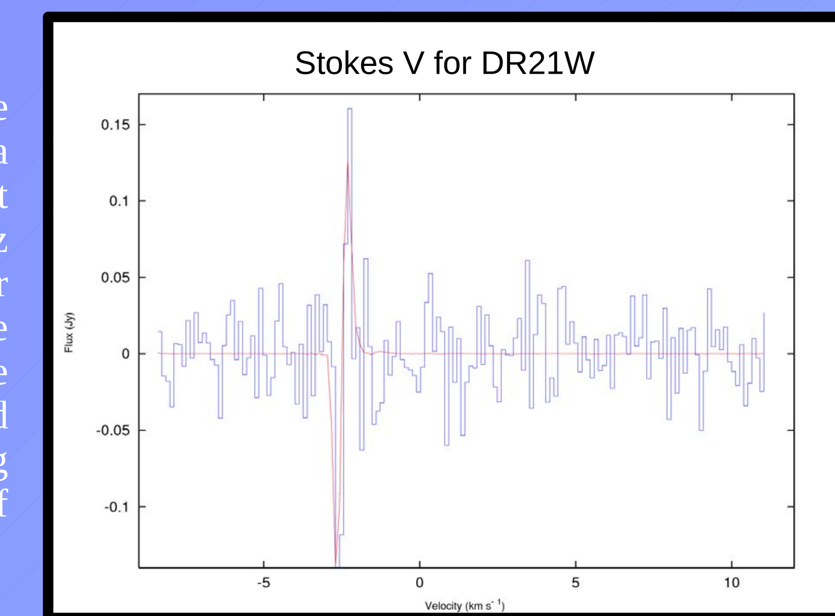

In the figure to the right, Stokes *V* (minus the scaled offset) for one source is plotted as a histogram against the best fit of the scaled derivative of Stokes *I*. A line-of-sight magnetic field can be obtained with the fit parameter *b* via the equation

$$b = zB\cos\theta$$

where *z* is the Zeeman splitting factor and $B\cos\theta$ is the line of sight magnetic field. Using the same value for *z* as Sarma and Momjian (1.7 Hz mg^{-1}), we detected a magnetic field of 58.09 ± 6.22 mG, which is 2-3 times stronger than that detected by Sarma and Momjian. Because a region's density is roughly proportional to the square of its magnetic field, this measurement places the lower density limit around 10^{10} cm^{-3} (Crutcher, 1999). Class I masers are expected to be found in regions of up to 10^6 mG.

Pumping Mechanisms

The currently accepted mechanism for Class I maser excitation is collisional pumping followed by radiative decay. When the molecules are collisionally excited, they spontaneously decay into an intermediate energy state. This creates the population inversion. However, this is though to occur in areas of lower density than seen in our data for DR21W.

An alternative to collisional pumping is collision-collision pumping, as proposed by Strelnistki (1993). In this pumping scheme, species with two different temperatures collide within the same cloud. Collisions with the warmer species cause the excitation, and collisions with the cooler species would cause the energy sink back to the intermediate level, creating a population inversion. This scheme has no density limits, and conditions would be right for this mechanism within outflows, where Class I masers are generally found.

Remarks

In several places, the 36 GHz masers align with masers detected in other transitions. In DR21OH, the masers in all transitions follow the same outflow pattern with similar velocities and positions. However, 44 GHz masers also appear scattered in the north and south while the 36 GHz are only in the south. In some cases, the two transitions align very closely, but in others they are separated. In DR21W, the three transitions align in one corner, but only the 36 GHz masers appear to the south. The differences in conditions required for different maser transitions is still fairly uncertain.

Acknowledgments

The REU program at MIT Haystack Observatory is funded by a grant from the National Science Foundation. Thanks to my mentor, Vincent Fish for his help and support, as well as everyone else who contributed to this project's analysis: Preethi Pratap, Ylva Pihlstrom, Vladimir Strelnitski, and Lorant Sjouwerman.

References

Araya, E.D., Kurtz, S., Hofner, P., Linz, H. 2009, ApJ, 698, 1329
Batrla, W. & Menten, K.M. 1988, ApJ, 329, L117
Crutcher, R.M. 1999, ApJ, 520, 706
Kogan, L. & Slysh, V. 1998, ApJ, 497, 800
Kumar, M. S. N., Davis, C. J., Grave, J. M. C., Ferrerira, B., & Froebrich, D. 2007, MNRAS, 374, 54
Müller, H. S. P., Menten, K. M., & Mäder H. 2004, A&A 428, 1019
Plambeck, R.L. & Menten, K.M. 1990, ApJ, 364, 555
Pratap, P., Shute, P.A., Keane, T.C., Battersby, C., & Sterling, S. 2008, ApJ, 135, 1718
Sarma, A.P. & Momjian, E. 2009, ApJ, 705, L176
Strelnitski, V. 1984, MNRAS, 207, 339